High-fidelity time-Stepping for reverse-time migration

Ben D. Wards, Gary F. Margrave, and Michael P. Lamoureux

ABSTRACT

As a result of the numerical performance of finite-difference operators, reverse-time migration (RTM) images are typically low frequency. This occurs because finite-difference operators must be oversampled to control numerical dispersion. We consider a high-fidelity time-stepping equation based on the Fourier transform, which is exact if an aliasing condition is met. The technique is adapted to variable velocity using a localized Fourier transform (Gabor transform). The feasibility of using the time-stepping equation for RTM is demonstrated by studying its stability properties, its impulse response, and by migrating a synthetic example of a salt dome. We show that a high frequency wavefield can be time stepped with no loss and with a much larger time step than commonly used.

INTRODUCTION

Reverse-time migration (RTM) is a very powerful depth migration algorithm. It is capable of imaging reflectors using overturned waves and multiples. However, especially for large prestack 3D seismic processing, the computational time and input/output memory costs can be prohibitively expensive. As a result, images usually contain only low frequencies. An example of the impressive performance, yet low frequency response, of the method is Jones et al. (2007).

McMechan (1983) describes a poststack RTM algorithm called "boundary value migration". The stacked recorded wavefield is treated as a time-dependent boundary condition at the surface of the model. Migration is performed by pushing the recorded wavefield backwards in time into the subsurface with half the modelling velocity. The recorded wavefield is propagated backwards to time $t = 0$. The specification of this time is referred to as the the imaging condition, the time at which the reflection events occur. Independently, Whitmore (1983) and Baysal et al. (1983) developed the same method, called backward-time propagation and RTM, respectively. RTM can be thought of as the inverse operation of forward modelling. The acoustic wave equation is symmetric about a reverse in the time coordinate. This implies that the same finite-difference code that is used for forward modelling can be used for inverse modelling.

RTM was adapted for prestack migrations by the development of an imaging condition for acoustic waves (Chang and McMechan, 1986). This imaging condition is essentially the same as that originally proposed by Claerbout (1971). In prestack RTM, typically, a shot model is forward propagated by finite-differencing the wave equation, and the receiver field is similarly back propagated. The imaging condition is applied to the shot and receiver fields to determine when a reflection event occurs. RTM is used when conventional algorithms fail to resolve complex targets. This often occurs when attempting to image structures like salt domes and highly faulted terrain (Whitmore and Lines, 1986).

Prestack RTM is a less commonly used migration algorithm because finite-difference operators must be finely sampled in space and time. As a result of the sampling require-

ments, processing 3D seismic surveys will either require harsh filtering to remove higher frequency data or they will require unacceptably long run times even with a cluster of computers. The fine sampling requirements occur because finite-difference operators propagate high frequencies with an incorrect dispersion relation.

We propose an alternative time-stepping equation that does not use finite differences. The equation can time-step a wavefield using a coarser time step because the spatial derivatives in the wave equation are computed exactly in the Fourier domain and so do not suffer from dispersion at high frequencies. As a result, the sampling requirements are better than propagating with finite differences. The fundamental limitation on the time-step size in our method arises from a temporal aliasing condition, which we derive. The accuracy and stability properties are demonstrated by comparing solutions of the time-stepping equation to finite-difference solutions.

TIME STEPPING BY A PHASE-SHIFT INTEGRAL

A time-stepping equation is formulated by phase-shifting the Fourier transform of the wavefield by a cosine operator. The time-stepping equation is based on an exact solution of the homogeneous (constant velocity) wave equation,

$$U_{xx} + U_{zz} = \frac{1}{c^2} U_{tt}, \tag{1}$$

where U is the amplitude of the wave, x is the lateral coordinate, z is the depth coordinate, t is the time coordinate, and c, a constant, is the speed of propagation. Assume $(x, z) \in \mathbb{R}^2$ and $t \in \mathbb{R}$, where $\mathbb{R}$ denotes the real numbers.

The Fourier transform over the spatial dimensions $\vec{x} = (x, z)$ transforms equation (1) into an ordinary differential equation,

$$-(k_x^2 + k_z^2)\hat{U} = \frac{1}{c^2}\hat{U}_{tt}, \tag{2}$$

where

$$\hat{U} = \hat{U}(\Delta t, \vec{k}) = \int_{\mathbb{R}^2} U(\Delta t, x, z) e^{i\vec{k}\cdot\vec{x}} dx dz, \tag{3}$$

and $\vec{k} = (k_x, k_z)$ are the wavenumbers which correspond to the coordinates $\vec{x} = (x, z)$. When $\vec{k} \neq 0$ equation (2) has the general solution,

$$\hat{U}(\Delta t, \vec{k}) = A(\vec{k}) e^{-i\Delta t\omega(\vec{k})} + B(\vec{k}) e^{i\omega(\vec{k})t}, \tag{4}$$

where $A(\vec{k})$ and $B(\vec{k})$ are dependent on the initial conditions, and wavenumber dependent frequency ω is determined from the dispersion relation

$$\omega(\vec{k}) = c\sqrt{k_x^2 + k_z^2}. \tag{5}$$

After the functions A and B are specified, the space domain solution may be calculated by taking an inverse Fourier transform. The space domain solution is then,

$$U(\Delta t, x, z) = \frac{1}{(2\pi)^2} \int_{\mathbb{R}^2} \{A(\vec{k}) e^{-i\Delta t\omega} + B(\vec{k}) e^{i\Delta t\omega}\} e^{i\vec{k}\cdot\vec{x}} dk_x dk_z. \tag{6}$$

Suppose the initial conditions $U(0,x,z) = f(x,z)$, $U_t(0,x,z) = g(x,z)$ hold for equation (1). Let $\hat{f}$ and $\hat{g}$ be the Fourier transform of f and g, respectively. Solving equation (2) for the initial conditions gives $2A(\vec{k}) = \hat{f}(\vec{k}) + \frac{\hat{g}(\vec{k})}{i\omega(\vec{k})}$ and $2B(\vec{k}) = \hat{f}(\vec{k}) - \frac{\hat{g}(\vec{k})}{i\omega(\vec{k})}$. Since it is difficult to obtain an accurate estimate of the first derivative of the wavefield, we eliminate g by considering the wavefield at two separate times. Then

$$\begin{aligned} 2U(\Delta t,x,z) + 2U(-\Delta t,x,z) = & \frac{1}{(2\pi)^2}\int\left(\hat{f}(\vec{k}) + \frac{\hat{g}(\vec{k})}{i\omega(\vec{k})}\right)e^{-i\Delta t\omega}e^{i\vec{x}\cdot\vec{k}}dk_xdk_z \\ & + \frac{1}{(2\pi)^2}\int\left(\hat{f}(\vec{k}) - \frac{\hat{g}(\vec{k})}{i\omega(\vec{k})}\right)e^{i\Delta t\omega}e^{i\vec{x}\cdot\vec{k}}dk_xdk_z \\ & + \frac{1}{(2\pi)^2}\int\left(\hat{f}(\vec{k}) + \frac{\hat{g}(\vec{k})}{i\omega(\vec{k})}\right)e^{i\Delta t\omega}e^{i\vec{x}\cdot\vec{k}}dk_xdk_z \\ & + \frac{1}{(2\pi)^2}\int\left(\hat{f}(\vec{k}) - \frac{\hat{g}(\vec{k})}{i\omega(\vec{k})}\right)e^{-i\Delta t\omega}e^{i\vec{x}\cdot\vec{k}}dk_xdk_z \\ = & \frac{1}{(2\pi)^2}\int 2\hat{f}(\vec{k})\left(e^{i\Delta t\omega} + e^{-i\Delta t\omega}\right)e^{i\vec{x}\cdot\vec{k}}dk_xdk_z \\ = & \frac{1}{(2\pi)^2}\int 4\hat{f}(\vec{k})\cos(\omega\Delta t)e^{i\vec{x}\cdot\vec{k}}dk_xdk_z. \end{aligned} \tag{7}$$

Let FT and FT^{-1} represent the forward and inverse 2D Fourier transform, respectively. Then equation (7) can be rearranged,

$$U(\Delta t,x,z) = -U(-\Delta t,x,z) + 2FT^{-1}[\cos(\omega(\vec{k})\Delta t)FT[U(0,x,z)]]. \tag{8}$$

The time stepping equation, equation (8), is an exact solution to the constant velocity wave equation. Equation (1) is independent of time; therefore, equation (8) can be used recursively to calculate the wavefield at future times. For numerical computation, the Fourier transform in equation (8) is implemented with a fast Fourier transform. This can be done because the phase shift operator $\cos(\omega(\vec{k})\Delta t)$ is independent of the spatial coordinate $\vec{x}$.

The second order time and second order space finite-difference solution of the wave equation can be derived directly from equation (8). If the $\cos$ function is replaced by its power series expansion, then

$$\begin{aligned} U(\Delta t,x,z) &= -U(-\Delta t,x,z) + \\ &\quad +2FT^{-1}[1-(c\Delta t)^2(k_x^2+k_z^2+H.O.T.))FT[U(0,x,z)]] \\ &= -U(-\Delta t,x,z) + 2U(0,x,z) + (c\Delta t)^2(U_{xx}+U_{zz}) + H.O.T., \end{aligned} \tag{9}$$

where $H.O.T.$ refers to higher order terms.

To demonstrate effectiveness of recursively using equation (8) for wavefield propagation, an impulse response and the response a minimum phase wavelet are stepped forward in time.. The impulse and minimum phase wavelet are injected at the center point of the model at the start of propagation. The exact solution is known for the impulse response, and is the Green's function solution to the 2-dimensional wave equation,

$$G(t,\vec{x};\tau,\vec{y}) = \frac{H(t-\tau-r)}{2\pi\sqrt{(t-\tau)^2-r^2}}, \tag{10}$$

where H is the Heaviside step function, $r = ||\vec{x}-\vec{y}||$ and $||\vec{x}|| = \sqrt{(x_1^2+x_2^2)}$ is the Euclidean norm. Figure 1 is the impulse response. The finite-difference solution contains

unacceptable high frequency noise arising from the dispersive propagation of the higher frequencies of the impulse. The response of the phase-shift time-stepping equation shows no dispersion and agrees with Green's function much better (Figure 2). The impulse response for finite-difference time stepper will never be good regardless of the time step because an impulse will always contain higher frequencies that a finite-difference operator can propagate. Figure 3 shows the propagation of an impulse using our Fourier time-stepper and also with conventional second-order finite differencing.. In spite of a much smaller time step, the finite-difference solution is still noisy.

The stability or aliasing condition constrains the temporal sampling of the wavefield. Equation (8) takes the wavefield at two distinct times with spatial sampling rate Δx and generates a new wavefield at a future time. The wavenumber which corresponds to the greatest frequency occurs when $\vec{k} = (\frac{1}{2\Delta x}, \frac{1}{2\Delta x})$, the Nyquist wavenumbers. By the dispersion relation shown in equation (5), this maximum wavenumber generates a frequency $\omega = \frac{1}{\sqrt{2}\Delta x}$. Since the wavefield is sampled in time at rate Δt, to avoid aliasing the frequencies generated from equation (5), the inequality $\omega < \frac{1}{\sqrt{2}\Delta t}$ must be satisfied, or equivalently

$$\frac{\Delta t\, c}{\Delta x} < \frac{1}{\sqrt{2}}. \tag{11}$$

The number $r = \frac{\Delta t\, c}{\Delta x}$ is commonly referred to as the Courant number and is a quantity that determines stability for a large number of finite-difference solvers. To demonstrate the instability implied by equation (11), a minimum phase wavelet is injected into a model at the center point and stepped forward in time using equation (8). The response can be observed in Figure 4 with Courant numbers close to the stability threshold. When equation (11) is satisfied the model is stable. When r is slightly greater than $1/\sqrt{2}$, instability is observed at high frequencies that are 45 degrees from the grid. When r is significantly greater than $1/\sqrt{2}$, instability is observed at all angles and at lower frequencies. While it is probably more correct to call this effect aliasing, we have used the more standard term "instability".

VARIABLE VELOCITY TIME STEPPING EQUATION

In RTM it is necessary to propagate a wavefield in a variable velocity medium. To demonstrate how equation (8) can be adapted to a variable velocity model, we consider a $v(z)$ medium where the velocity only varies in the vertical direction. In principle, a similar construction where the windowing functions depends in the x or lateral coordinate can be used for a general velocity model. At present, our construction smooths the velocity model and therefore is not capable of reflecting energy. This implies that it cannot account for multiples. Consider the set of windowing functions $\{\exp(-\frac{(z-an)^2}{2\sigma^2}), n = 1, ..., N\}$. This set of functions can be normalized to form a partition of unity,

$$\Omega_n(z) = \frac{e^{-\frac{(z-an)^2}{2\sigma^2}}}{\sum_{n=1}^{N} e^{-\frac{(z-an)^2}{2\sigma^2}}}, \quad n = 1 \ldots, N, \tag{12}$$

where $\sum_{n=1}^{N} \Omega_n(z) = 1$ for $0 \le z \le z_{max}$ and $0 \le \Omega_n \le 1$. The constants a, b, N, and σ are chosen so that the partition of unity covers the interval $[0, z_{max}]$. Additionally each

window Ω_n is localized at the point $z = a\,n$. The partition of unity is used to window the wavefield into regions. Each region is then propagated with a constant velocity v_n. This is done by multiplying the window by each vertical trace in the wavefield. A partition of unity with 8 windows is displayed in Figure 6. The time stepper, equation (8), can then be rewritten as

$$U(\Delta t, x, z) = -U(-\Delta t, x, z) + \sum_{n=1}^{N} 2FT^{-1}[\cos(\omega_n(\vec{k})\Delta t)FT[\Omega_n(\vec{x})U(0, \vec{x})]], \qquad (13)$$

where $\omega_n(\vec{k}) = v_n\sqrt{k_x^2 + k_z^2}$ and $\Omega_n(\vec{x}) = \Omega_n(z)$.

EXAMPLE

Firstly, equation (13) is used to forward model the response to a minimum phase wavelet in linear velocity medium. The wavelet is injected at 5 points marked with a hash. Analytically, the wavefront is a circle whose center of radius moves down in depth with time. Figure 5 is the image of response with velocity model $v(z) = 1.5\,z + 1000$. The response has good continuity and shows amplitude gradients along the wavefront as expected from geometric spreading despite the fact that there were only 11 windows used in the propagation.

Secondly, equation (13) is used for migrating a synthetic model of a salt dome by a poststack RTM. For comparison, the model is also migrated by finite differencing the wave equation. Poststack RTM is not expected to be useful migration algorithm because it cannot overcome the crude approximation of stacking complex structures. However, it is theoretically simple and is an useful exercise in order to demonstrate the feasibility of using equation (13) to do a prestack RTM. To generate a synthetic model of the salt dome, an acoustic finite-difference exploding reflector code was used. At time $t = 0$, all reflectors are simultaneously excited and the model is propagated forward using standard finite-difference modelling. The reflectors are represented by discontinuities in the velocity model. The wavefield is recorded at the surface of the model to produce a poststack seismic record. The seismic record is displayed in Figure 8 for the velocity model in Figure 7. The high constant velocity salt dome is on the right side of the velocity model. While on the left, the velocity model has a nonzero constant gradient. Figure 9 contains an image of the migrated synthetic model using finite differences. Figure 10 is the image of the migrated salt dome using the phase-shift time stepping equation. Both methods have produced an acceptable image of the salt dome although the finite-difference method required finer spatial sampling and finer time-stepping. The finite difference code operated with the grid spacing of $\Delta x = 2.5$, and resampled the time increment to $\Delta t = 0.0002s$, and the runtime was 2 hours and 10 minutes. For the phase-shift time stepping equation, $\Delta x = 10m$, the time coordinate was resampled to $\Delta t = 0.004s$, and the runtime was 14 minutes using 22 windows.

CONCLUSION

We proposed a Fourier domain time-stepping equation for RTM which is used to migrate a poststack image of a salt dome. Our method multiplies the spatial Fourier transform of the wavefield by a cosine whose argument depends on velocity and wavenumber. This

can be interpreted as a spatial phase shift. For comparison the salt dome was migrated by finite-difference time stepping the full wave equation. The two images were comparable in quality and the phase-shift time-stepping equation was computed in a fraction of the time. As a result of computing the phase shift time-stepping equation in the Fourier domain, a much larger time step is possible then by using finite-differences. The phase-shift time-stepping equation is an exact solution to the homogeneous wave equation. It was adapted to the nonhomogeneous wave equation by windowing the wavefield and propagating within each window as a homogeneous medium. This windowing process prevents the reflection of energy at any interface in the velocity model and therefore it cannot be used to image multiples directly. The phase-shift time stepping equation has practically no dip limitation and therefore it can correctly propagate overturned waves. As a result of the larger time step, the phase-shift time-stepping equation can, in principle, be used to make higher fidelity seismic images. A stability condition was derived based on an aliasing condition between space and time domains. Numerical examples support the stability condition. The impulse response of a delta function to the phase-shift time-stepping equation matches the theoretical Green's function almost exactly while the response to the finite-difference solution contained spurious noise.

FUTURE WORK

Future work will develop an optimal method of windowing the data. Current work indicates that under a large choice of windows the output is similar. We windowed the data before propagation but it is also possible to window after and/or before propagation. The phase-shift equation cannot account for a velocity gradients without using finely spaced windows or reflection interfaces. Therefore, future work will attempt to adjust the time-stepping equation to account for these phenomena. Conceptually, there is no difference between forward or backpropagating shot and receiver fields for prestack RTM versus back propagating a stacked section. Hence, the phase-shift time-stepping equation is expected to be directly applicable to prestack RTM. However, future work is required to evaluate the phase-shift time stepping equation on acquired seismic data and more complicated synthetic models for poststack and prestack RTM.

REFERENCES

Baysal, E., Kosloff, D. D., and Sherwood, J. W. C., 1983, Reverse time migration: Geophysics, **48**, No. 11, 1514–1524.

Chang, W.-F., and McMechan, G. A., 1986, Reverse-time migration of offset vertical seismic profiling data using the excitation-time imaging condition: Geophysics, **51**, No. 1, 67–84.

Claerbout, J. F., 1971, Toward a unified theory of reflector mapping: Geophysics, **36**, No. 3, 467–481.

Jones, I. F., Goodwin, M. C., Berranger, I. D., Zhou, H., and Farmer, P. A., 2007, Application of anisotropic 3d reverse time migration to complex north sea imaging: SEG Technical Program Expanded Abstracts, **26**, No. 1, 2140–2144.

McMechan, G. A., 1983, Migration by extrapolation of time-dependent boundary values: Geophysical Prospecting, **31**, No. 3, 413–420.

Whitmore, N. D., 1983, Iterative depth migration by backward time propagation: SEG Technical Program Expanded Abstracts, **2**, No. 1, 382–385.

Whitmore, N. D., and Lines, L. R., 1986, Vertical seismic profiling depth migration of a salt dome flank: Geophysics, **51**, No. 5, 1087–1109.

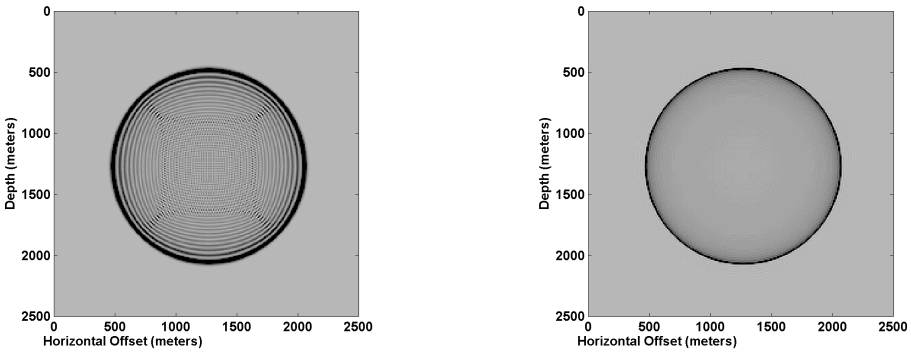

(a) (b)

FIG. 1. (a) The impulse response for finite-differencing the wave equation with $\Delta t = 0.00005$. (b) The impulse response for the phase-shift time-stepping equation where $\Delta t = 0.001$.

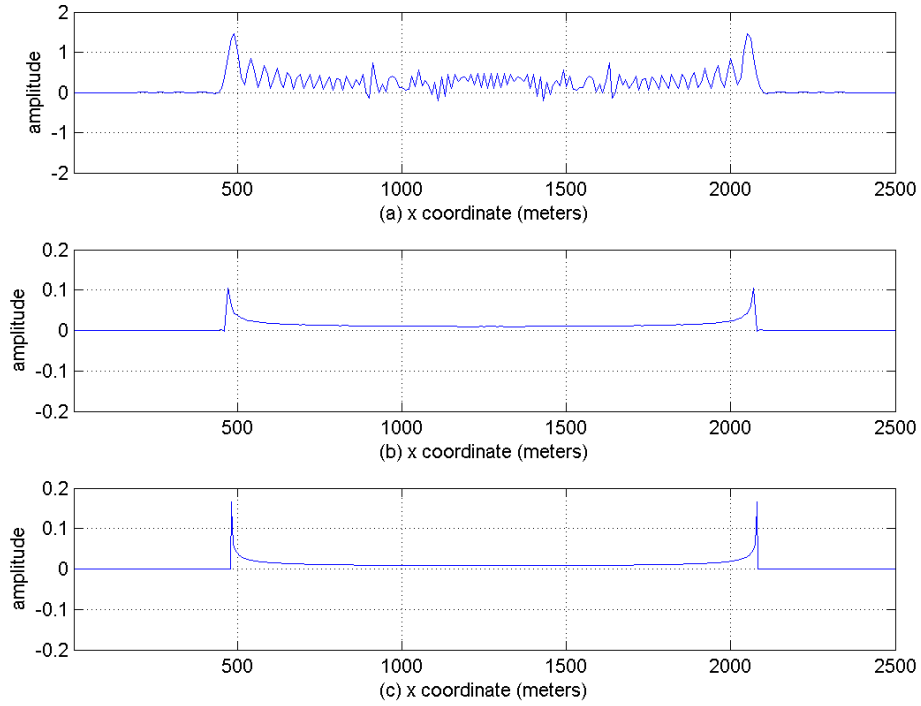

FIG. 2. Cross Section of wavefields in Figure 1 (a) using finite differences, and (b) using the phase-shift time-stepping equation. In (c) is shown the exact Green's function.

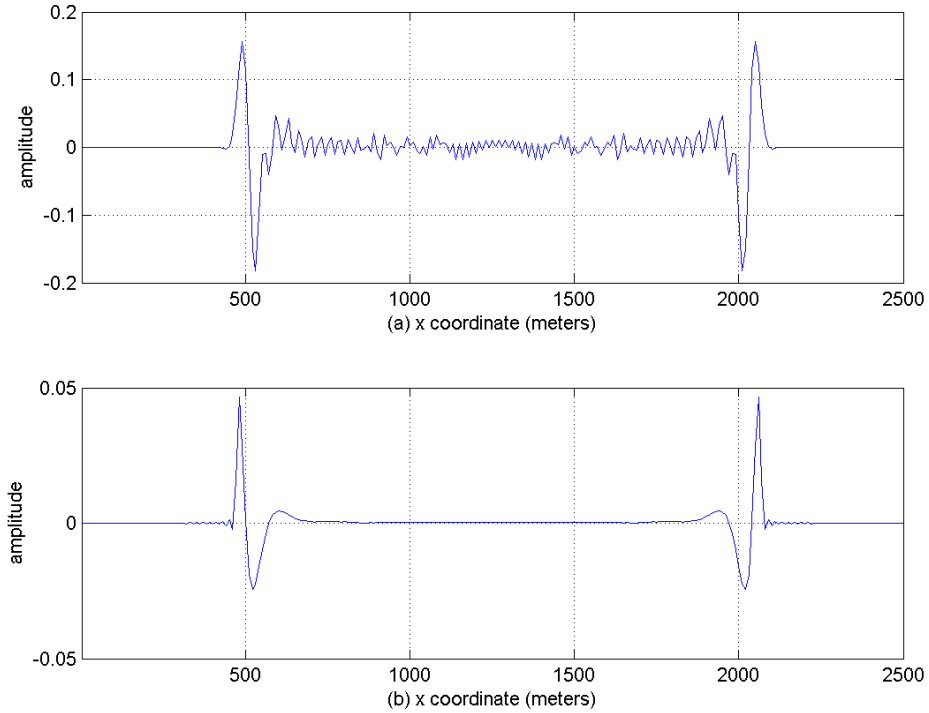

FIG. 3. Cross Section through center of model of the response to a minimum phase wavelet injected at the center the model. (a) using finite differences with $\Delta t = 0.0001$. (b) using phase-shift time stepping equation with $\Delta t = 0.001$. The finite-difference time-stepper took 10 times as long to execute.

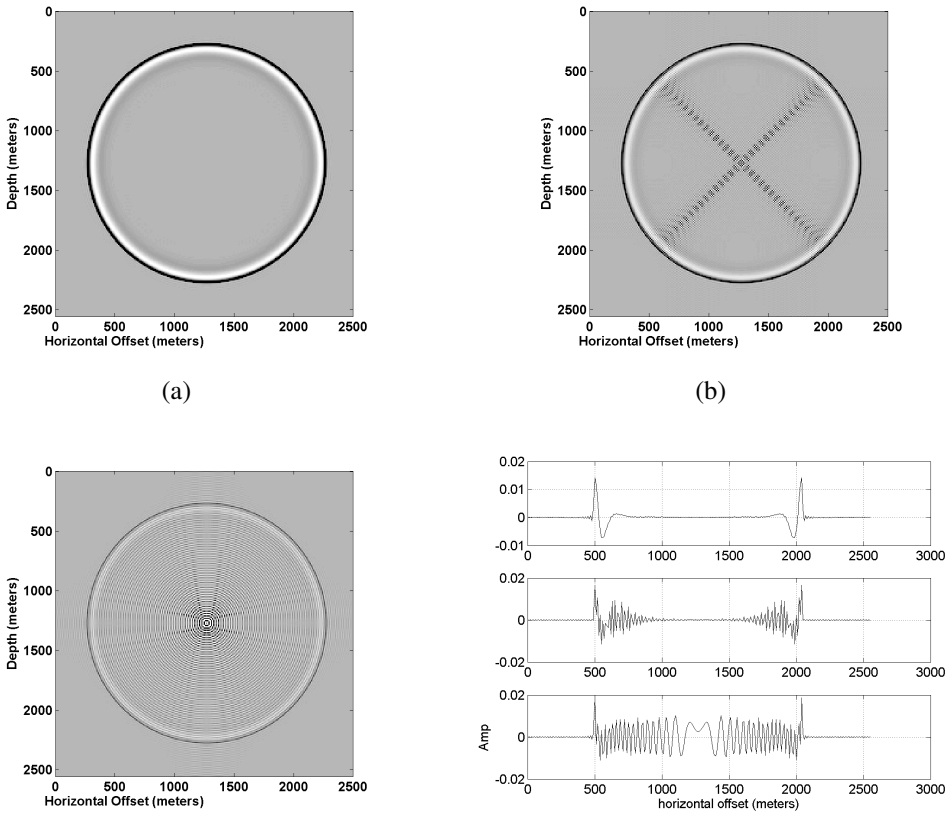

FIG. 4. Response to minimum phase wavelet injected at the center of a constant velocity model and forward propagated for various values of the Courant number r. When $r > 1$ aliasing occurs in the model and the model is unstable. (a) The Courant number $r = 0.60 \leq 0.71$. The model is correctly forward propagated. (b) The Courant number $r = 0.80 \not\leq 0.71$. Instability is observed when both wavenumbers are large. (c) The Courant number $r = 1.00 \not\leq 0.71$. Any large wavenumber is unstable. Noise occurs through out the model. (d) Cross sectional view in the horizontal direction. Graphs from top to bottom correspond to Figures (a), (b), and (c).

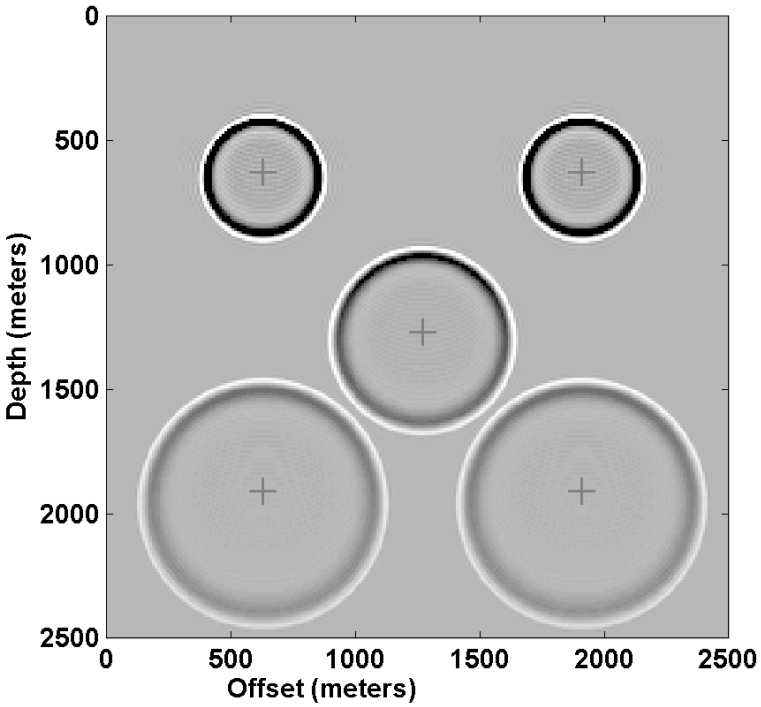

FIG. 5. Minimum phase wavelet injected at the center of the model with velocity $v(z) = 1.5s^{-1}\, z + 1000m\, s^{-1}$. There were 11 windows used for propagation with $\Delta t = 0.0015s$ and $\Delta x = 10m$.

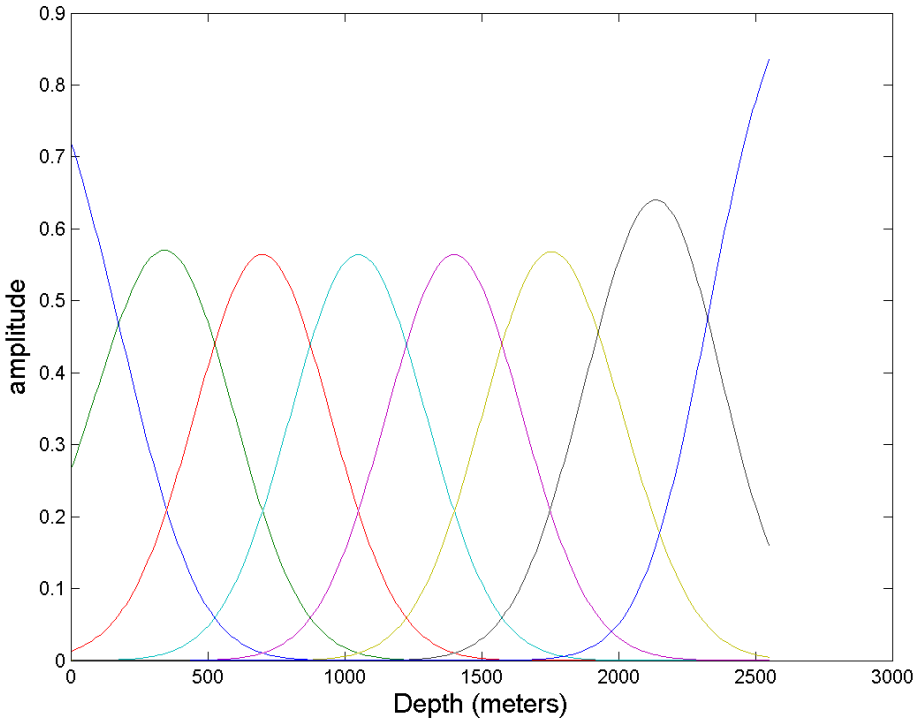

FIG. 6. A set of Gaussian windowing functions. No windows appear at the end of the domain to act as padding.

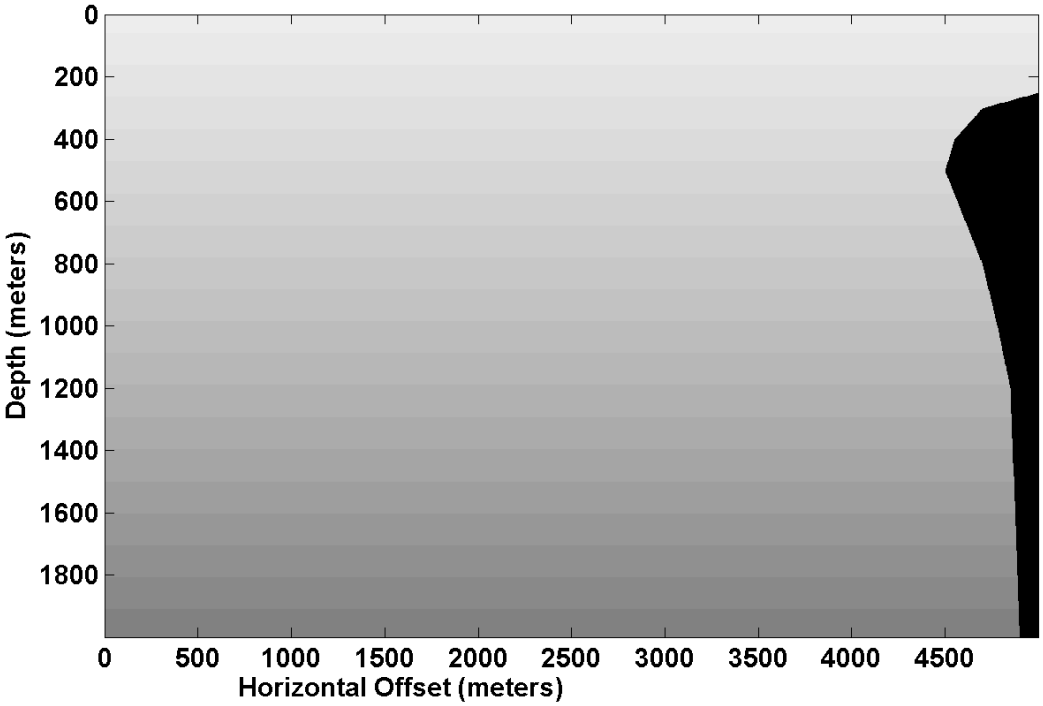

FIG. 7. The Velocity Model of a Salt Dome. The velocity of the salt dome is $5000ms^{-1}$, and the velocity of the region to the left of the saltdome is $v(z) = 1500ms^{-1} + 0.8s^{-1}z$

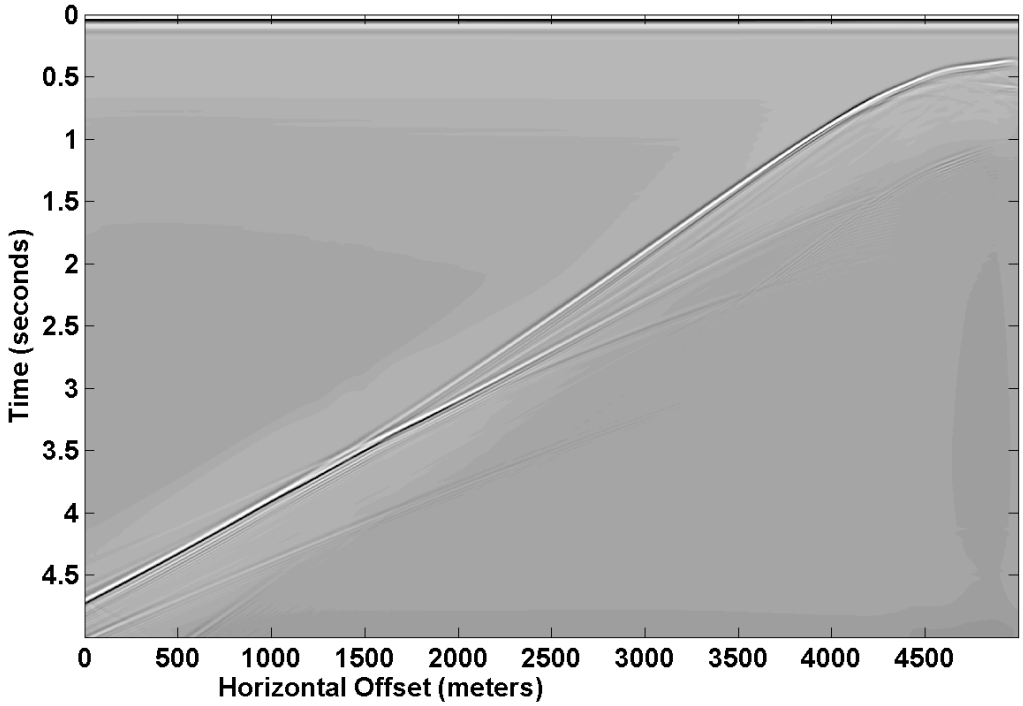

FIG. 8. The Exploding Reflector Model of the Salt Dome

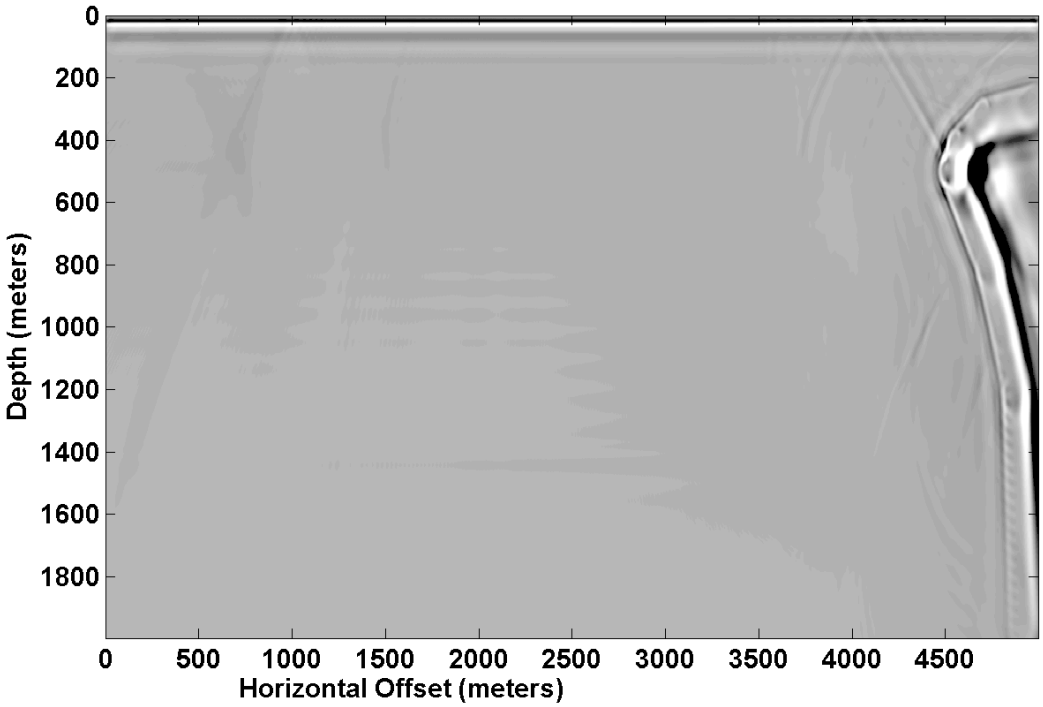

FIG. 9. The Migrated Salt Dome using a finite-difference time stepper with $\Delta x = 2.5m$ and $\Delta t = 0.0002s$

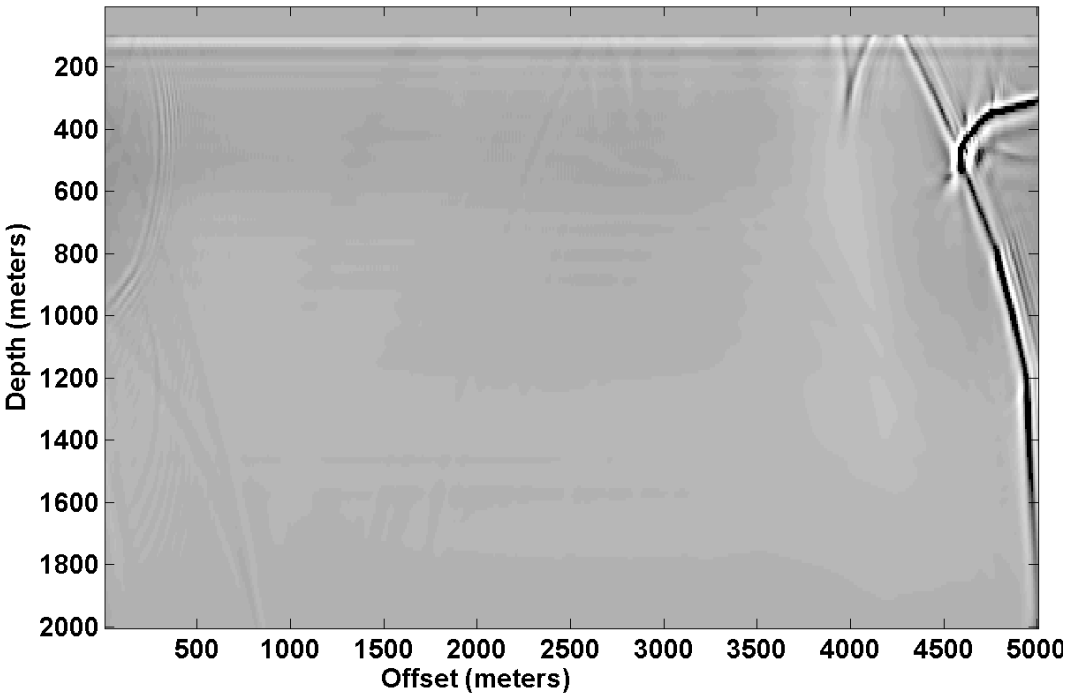

FIG. 10. The migrated salt dome using the phase shift timestepper with $\Delta x = 10m$ and $\Delta t = 0.004s$.